

## Noble gas signatures of Antarctic nakhlites, Yamato (Y) 000593, Y000749, and Y000802

Ryuji Okazaki<sup>1\*</sup>, Keisuke Nagao<sup>1</sup>, Naoya Imae<sup>2</sup> and Hideyasu Kojima<sup>2</sup>

<sup>1</sup> *Laboratory for Earthquake Chemistry, University of Tokyo, Hongo, Bunkyo-ku, Tokyo 113–0033*

<sup>2</sup> *Antarctic Meteorite Research Center, National Institute of Polar Research,  
Kaga 1-chome, Itabashi-ku, Tokyo 173–8515*

**Abstract:** We have measured noble gases in three nakhlites from Antarctica, Yamato (Y) 000593, Y000749, and Y000802, by step-heating and total-melting methods. The trapped  $^{36}\text{Ar}/^{84}\text{Kr}/^{132}\text{Xe}$  ratios determined for the bulk samples are around 80/3/1, identical to those of Nakhla. The Yamato nakhlites also release noble gases showing high  $^{129}\text{Xe}/^{132}\text{Xe}$  (up to 1.486) and low  $^{84}\text{Kr}/^{132}\text{Xe}$  (~1.5) at 1000 and 1300°C, which is one of the most characteristic signatures of nakhlites. The low  $^{84}\text{Kr}/^{132}\text{Xe}$ , as compared to that of the Mars atmosphere, suggests the presence of a fractionated Martian atmosphere.

Cosmic-ray exposure ages based on cosmogenic  $^{21}\text{Ne}$  are 11.7, 11.9, and 13.0 Ma for Y000593, Y000749, and Y000802, respectively. This supports the pairing based on the mineralogical and petrographical similarities and the location of the finds. The average of the  $^{21}\text{Ne}$  exposure ages is  $12.05 \pm 0.69$  Ma. We also calculated an apparent  $^{81}\text{Kr}$ -Kr age as  $11.8 \pm 1.0$  Ma from cosmic-ray produced radioactive  $^{81}\text{Kr}$  and stable Kr isotopes from Y000593. The coincidence with the  $^{21}\text{Ne}$  exposure age indicates a short terrestrial age ( $< 0.04$  Ma). Hence, the Mars ejection time, as calculated from the sum of the  $^{21}\text{Ne}$  exposure age and terrestrial age, is  $12.1 \pm 0.7$  Ma. Calculated K-Ar gas retention age for the Yamato nakhlites is  $1.24 \pm 0.22$  Ga. The ejection time and gas retention age are close to those of non-Antarctic nakhlites and Chassigny. This suggests that the Yamato nakhlites were ejected from Mars together with other nakhlites and Chassigny.

Xenon isotopes are mixtures of Chassigny Xe, fission Xe, and the Mars atmosphere. High-temperature fractions (1000–1750°C) are enriched in the Mars atmosphere and fission Xe components, compared to lower temperature fractions. There are similarities in Xe isotopes between Y000749 and Y000802 showing excesses in  $^{129}\text{Xe}$  and  $^{136}\text{Xe}$ , whereas Y000593 has only small excesses. The release pattern of  $^{130}\text{Xe}$  for Y000593 is also different from those of the other two nakhlites. A mineralogical study pointed out that Y000593 has lower olivine abundance compared to the others. These differences in Xe isotopes and petrologic features probably represent the heterogeneities of the ejection site on Mars.

**key words:** Martian meteorite, trapped noble gas, cosmic-ray exposure age, terrestrial age, K-Ar gas retention age

\* Present address: Department of Geological Sciences, Arizona State University, P.O. Box 871404, Tempe, AZ 85287-1404, U.S.A.

Corresponding author: R.O. (Fax: +81-3-5841-4119, E-mail: okazaki@eqchem.s.u-tokyo.ac.jp)  
(Fax: +1-480-965-8102, Phone: +1-480-965-3523, E-mail: okazaki@asu.edu)

## 1. Introduction

Japanese Antarctic Research Expedition in 2000 (JARE-41) found over 3500 meteorite specimens in the Yamato meteorite field. Among them, a heavy achondrite, Yamato (Y) 000593 (13.7 kg) was recognized to be a nakhlite from petrological and mineralogical features (Kojima and Imae, 2001; Imae *et al.*, 2002, 2003). Two stones (Y000749 of 1.3 kg and Y000802 of 22 g) were found nearby, and they are probably paired with the Y000593 meteorite based on petrographical and mineralogical similarities and the locations of the finds (Kojima and Imae, 2001; Kojima *et al.*, 2002; Imae *et al.*, 2002, 2003).

Nakhlites are one of the SNC meteorite members named after three meteorites, Shergotty, Nakhla, and Chassigny. Shergottites are basaltic rocks, whereas nakhlites and Chassigny have features of plutonic cumulates (*e.g.*, McSween, 1994). The SNCs were initially classified as HED (Howardite-Eucrite-Diogenite) meteorites because of their similarities in mineralogical and petrological features. It was recently shown that SNCs are obviously different from HEDs in crystallization ages (Geiss and Hess, 1958; Gale *et al.*, 1975; McSween, 1994), and oxygen (Clayton and Mayeda, 1996), nitrogen (Becker and Pepin, 1984; Wiens *et al.*, 1986), and noble gas (Pepin, 1985) isotopic compositions. After that, SNC meteorites were reconsidered, and thought to have formed on a parent body different from that of the HED members: most plausibly “Mars.” Some of the strongest evidence for the Martian origin of SNC meteorites is the excellent coincidence in abundances of noble gas and other volatile elements between impact-melt glasses of the EET79001 shergottite (Pepin, 1985) and Viking probe data (Owen *et al.*, 1977) of the Martian atmosphere. This is supported by laboratory experiments suggesting that shock implantation does not cause significant elemental fractionation of noble gases (Bogard *et al.*, 1986; Wiens and Pepin, 1988). Mars atmospheric noble gas ratios have been repeatedly compared with data of impact glasses of EET79001 and impact veins of Zagami, and are estimated to be  $20.5 \pm 2.5$  and  $2.60 \pm 0.05$  for  $^{84}\text{Kr}/^{132}\text{Xe}$  and  $^{129}\text{Xe}/^{132}\text{Xe}$ , respectively (Bogard and Garrison, 1998).

Noble gas data are useful to support SNC meteorite classification because there are variations in isotopic and elemental ratios of heavy trapped noble gases of Ar, Kr, and Xe. In addition to isotopic signatures, chronological constraints on the meteorite history are available from radiometric systems, such as  $^{39}\text{Ar}$ - $^{40}\text{Ar}$ ,  $^{40}\text{K}$ - $^{40}\text{Ar}$ ,  $^{129}\text{I}$ - $^{129}\text{Xe}$ , U-Th-He, and  $^{244}\text{Pu}$ -Xe. The duration of cosmic-ray exposure (CRE) in space can be also determined using cosmogenic isotopes.

Within the following, we will report the results of noble gas analyses for Y000593, Y000749, and Y000802. First, we will present signatures of trapped noble gases and discuss elemental and isotopic ratios. Second, we will estimate the timing of crystallization and ejection from Mars based on radiogenic  $^{40}\text{Ar}$  and cosmic-ray produced noble gases, respectively. Based on these noble gas data, we will confirm the classification and potential pairing predicted by the mineralogical study (Kojima and Imae, 2001; Kojima *et al.*, 2002; Imae *et al.*, 2002, 2003).

## 2. Samples and experimental methods

### 2.1. Experiments

Whole rock samples of about 200 mg were prepared from each meteorite for step-heating analyses. Noble gases were extracted from the samples in a Mo crucible by heating stepwise at 400, 600, 800, 1000, 1300, and 1750°C for 20 min. In addition to the step-heating analyses, a total-melting extraction (at 1750°C) was performed for Y000593 (0.2963 g) in order to determine a precise Kr-isotope data for  $^{81}\text{Kr}$ -Kr dating.

Extracted noble gases were purified through our standard procedure, and measured with a modified VG5400 mass spectrometer (MS-II) at the Laboratory for Earthquake Chemistry, University of Tokyo. Details of the analytical procedure and conditions of the MS-II are described in Nagao *et al.* (1999).

### 2.2. Partitioning of the noble gas components

Isotopic ratios of He, Ar, Kr, and Xe show that they are mixtures of cosmogenic, radiogenic, and trapped components. Neon is almost completely cosmogenic, although there is variation in  $^{21}\text{Ne}/^{22}\text{Ne}$  related with temperatures of the step-heating analyses (see Section 3.3). Assumptions for the partitioning of the cosmogenic (c) and trapped (t) components are as follows:  $^3\text{He}_t=0$ ,  $^{21}\text{Ne}_t=0$ ,  $(^{38}\text{Ar}/^{36}\text{Ar})_c=1.55$ ,  $(^{38}\text{Ar}/^{36}\text{Ar})_t=0.188$ . Contributions from trapped and fission components on Kr isotopes were corrected to determine cosmogenic Kr spectra for the  $^{81}\text{Kr}$ -Kr dating using the method described in Miura *et al.* (1993), assuming terrestrial atmosphere (Ozima and Podosek, 2002) as a trapped component. Trapped  $^{84}\text{Kr}$  concentrations were estimated from the following equation:

$$[^{84}\text{Kr}]_t = (^{84}\text{Kr}/^{83}\text{Kr})_t \cdot \frac{(^{86}\text{Kr}/^{83}\text{Kr})_c - (^{86}\text{Kr}/^{83}\text{Kr})_{m-f}}{(^{86}\text{Kr}/^{83}\text{Kr})_c - (^{86}\text{Kr}/^{83}\text{Kr})_t} \cdot [^{83}\text{Kr}]_m,$$

where  $(^{84}\text{Kr}/^{83}\text{Kr})_t=4.966$  (Earth Atm.),  $(^{86}\text{Kr}/^{83}\text{Kr})_c=0.0152$  (Marti and Lugmair, 1971), and  $(^{86}\text{Kr}/^{83}\text{Kr})_t=1.516$  (Earth Atm.). The  $[^{83}\text{Kr}]_m$  is the measured  $^{83}\text{Kr}$  concentration, while the  $(^{86}\text{Kr}/^{83}\text{Kr})_{m-f}$  is calculated by subtracting the fission  $^{86}\text{Kr}$  contribution from the measured  $(^{86}\text{Kr}/^{83}\text{Kr})_m$  based on the fission  $^{136}\text{Xe}$  abundance,  $[^{136}\text{Xe}]_f$ , and the  $^{244}\text{Pu}/^{238}\text{U}$  ratio of 0.0068 (Hudson *et al.*, 1989). In order to obtain the  $[^{136}\text{Xe}]_f$  and spallation-corrected Xe isotopic ratios, we used the spallation spectrum estimated from the Stannern eucrite (Marti *et al.*, 1966) and  $(^{126}\text{Xe}/^{130}\text{Xe})_t=0.0218$  (Earth Atm.; Ozima and Podosek, 2002).

## 3. Results and discussion

Table 1 shows concentrations and elemental ratios of trapped noble gases together with  $^{129}\text{Xe}/^{132}\text{Xe}$ . In the Appendix, we present full sets of noble gas data determined for the Yamato nakhlites. There are discrepancies in  $^{36}\text{Ar}_t$  concentration and  $(^{36}\text{Ar}/^{132}\text{Xe})_t$  between total-melting and step-heating analyses for Y000593. Heterogeneous distributions of  $^{36}\text{Ar}_t$  may be responsible for the differences between the two Y000593 samples. Alternatively, the correction of cosmogenic  $^{36}\text{Ar}$  for the total-melting data might be inappropriate, because the measured  $^{38}\text{Ar}/^{36}\text{Ar}$  ratio is close to the

Table 1. Concentrations and elemental ratios of trapped noble gases of Y000593, Y000749, and Y000802.

	$^{36}\text{Ar}_t$	$^{84}\text{Kr}_t$	$^{132}\text{Xe}_t$	$(^{36}\text{Ar}/^{132}\text{Xe})_t$	$(^{84}\text{Kr}/^{132}\text{Xe})_t$	$(^{129}\text{Xe}/^{132}\text{Xe})_t$
<i>Y000593 step heating (0.1622 g)</i>						
400°C	0.142 ±0.014	64.0 <sup>a)</sup> ±6.4	4.34 ±0.44	32.8 ± 4.7	14.7 ±2.1	1.038 ±0.027
600°C	0.0481 ±0.0070	12.3 <sup>a)</sup> ±1.2	2.67 ±0.28	18.0 ± 3.2	4.59 ±0.67	1.036 ±0.047
800°C	0.387 ±0.040	8.01 ±0.86	5.92 ±0.63	65.3 ± 9.8	1.35 ±0.21	1.021 ±0.043
1000°C	0.638 ±0.067	3.14 ±0.84	1.16 ±0.14	549 ± 88	2.70 ±0.79	1.16 ±0.10
1300°C	0.288 ±0.031	6.75 ±0.80	10.2 ±1.1	28.1 ± 4.3	0.66 ±0.10	1.092 ±0.048
1750°C	0.857 ±0.087	11.7 ±1.3	3.28 ±0.47	262 ± 46	3.58 ±0.64	1.16 ±0.13
total	2.36 ±0.24	106 ±11	27.6 ±2.8	85.4 ± 12.3	3.83 ±0.56	1.074 ±0.031
<i>Y000593 total melting (0.2963 g)</i>						
1750°C	0.904 ±0.096	153 ±15	38.0 ±8.4	23.8 ± 5.9	4.03 ±0.98	1.07 ±0.19
<i>Y000749 step heating (0.2048 g)</i>						
400°C	0.0972 ±0.0097	20.1 <sup>a)</sup> ±2.0	5.06 <sup>a)</sup> ±0.51	19.2 ± 2.7	3.97 ±0.56	1.050 ±0.044
600°C	0.0271 ±0.0028	4.73 <sup>a)</sup> ±0.47	3.25 <sup>a)</sup> ±0.33	8.3 ± 1.2	1.46 ±0.21	1.054 ±0.051
800°C	0.127 ±0.015	7.4 ±1.1	3.00 ±0.34	42.4 ± 6.9	2.48 ±0.45	1.109 ±0.073
1000°C	0.0616 ±0.0076	3.2 ±1.2	0.75 ±0.10	82 ± 15	4.2 ±1.7	1.44 ±0.15
1300°C	0.101 ±0.011	0.94 ±0.36	1.05 ±0.25	96 ± 25	0.90 ±0.40	1.44 ±0.30
1750°C	0.641 ±0.066	4.68 ±0.74	0.69 ±0.29	929 ±405	6.8 ±3.1	1.42 ±0.58
total	1.06 ±0.11	41.1 ±5.0	13.8 ±1.5	76 ± 11	2.98 ±0.48	1.133 ±0.050
<i>Y000802 step heating (0.1772 g)</i>						
400°C	0.159 ±0.016	36.0 ±3.7	9.61 <sup>a)</sup> ±0.96	16.5 ± 2.3	3.74 ±0.54	1.064 ±0.026
600°C	0.0400 ±0.0044	5.12 ±0.57	3.75 <sup>a)</sup> ±0.38	10.7 ± 1.6	1.37 ±0.21	1.127 ±0.043
800°C	0.431 ±0.044	5.33 ±0.59	3.35 ±0.35	128 ± 19	1.59 ±0.24	1.159 ±0.050
1000°C	0.173 ±0.019	2.41 ±0.50	1.65 ±0.18	105 ± 16	1.46 ±0.34	1.486 ±0.068
1300°C	0.287 ±0.030	2.58 ±0.34	2.01 ±0.26	143 ± 24	1.28 ±0.24	1.45 ±0.13
1750°C	0.516 ±0.052	4.76 ±0.52	0.517 ±0.093	997 ±205	9.2 ±1.9	1.31 ±0.22
total	1.60 ±0.16	56.2 ±5.8	20.9 ±2.1	77 ± 11	2.69 ±0.39	1.167 ±0.024

<sup>a</sup> Measured values are presented. Units for Ar and Kr-Xe are 10<sup>-9</sup> and 10<sup>-12</sup> cm<sup>3</sup> STP/g, respectively. Spallation-corrected  $^{129}\text{Xe}/^{132}\text{Xe}$  ratios are also shown. Presented errors were 1σ obtained from propagation of errors for concentrations (10%) and isotopic ratios.

assumed cosmogenic value (Appendix).

### 3.1. Trapped noble gas compositions of Y000593, Y000749, and Y000802

There is a wide diversity in noble gas elemental ratios in solar system reservoirs such as Sun, Venus, Mars, Earth, chondrites, and achondrites (Fig. 1). In the plot of  $^{84}\text{Kr}/^{132}\text{Xe}$  and  $^{36}\text{Ar}/^{132}\text{Xe}$ , we can see two trends, Sun-Venus-chondrite and Earth-Mars-achondrite lines. SNC meteorites and eucrites plot on the lower left of the Earth-Mars-achondrite line (Fig. 1). Noble gases of Chassigny are enriched in Xe, distinct from those of Nakhla, Shergotty, and the Mars atmosphere. Our data (Table 1) for Y000593, Y000749, and Y000802 plot close to Nakhla (total compositions of step-heating data are shown in Fig. 1). Hence, the noble gas elemental ratios are consistent with the classification of these meteorites as Nakhla-type Martian meteorites based on the petrological and mineralogical studies (Kojima and Imae, 2001; Kojima *et al.*, 2002; Imae *et al.*, 2002, 2003). Some eucrites (*e.g.*, Juvinas and Camel Donga; Miura *et al.*, 1998) have noble gas elemental ratios similar to those of nakhlites (Fig. 1), but the spread in the data for eucrites primary reflects addition of fractionated terrestrial atmosphere, as shown by Xe isotopic ratios (Miura *et al.*, 1998; Busemann and Eugster,

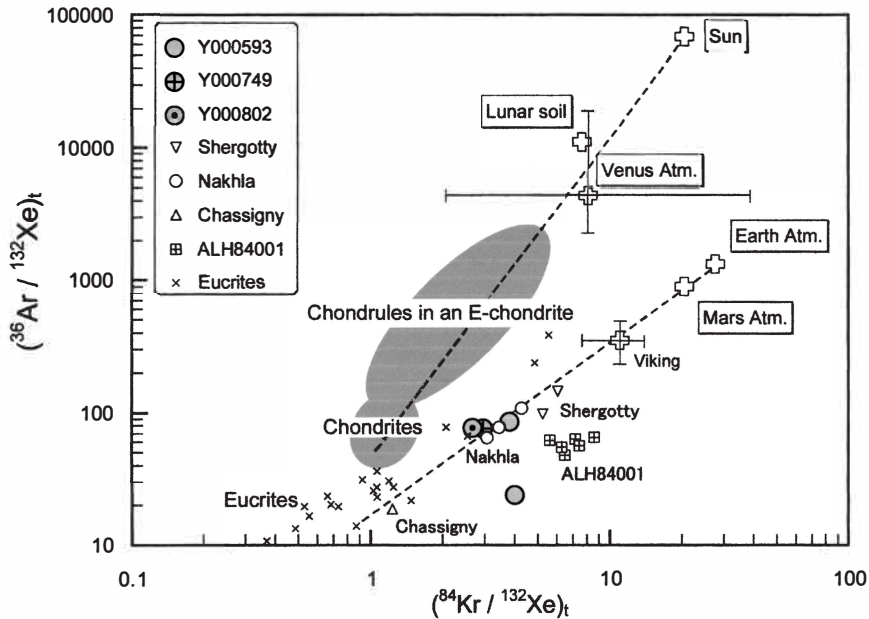


Fig. 1. Elemental ratios of trapped (primordial) noble gases in solar system reservoirs. Uncertainties approximately correspond to the size of the data markers, except for those of the Venus atmosphere and Viking data. Data sources: Sun (Anders and Grevesse, 1989); lunar soil (Eberhardt *et al.*, 1972); terrestrial atmosphere (Ozima and Podosek, 2002); Venusian atmosphere (estimated from Pepin (1991) assuming  $^{132}\text{Xe}/^{130}\text{Xe}=6.5$ ); chondrules in an E-chondrite (Okazaki *et al.*, 2001); Viking probe data (Owen *et al.*, 1977); Mars atmosphere (trapped gases in shergottite glasses; Bogard and Garrison, 1998); Shergotty, Nakhla, Chassigny (Otto, 1988); ALH84001 (Miura *et al.*, 1995; Bogard and Garrison, 1998); eucrites (Miura *et al.*, 1998).

2002). In addition, their crystallization ages of eucrites are older (close to those of Angra dos Reis of 4.5578 Ga; Lugmair and Galer, 1992) relative to those of nakhlites (~1.3 Ga; Nyquist *et al.*, 2001).

Excess  $^{129}\text{Xe}$  ( $^{129}\text{Xe}/^{132}\text{Xe} > 1$ ) is one of the most important features of Martian meteorites, except for Chassigny (Ott, 1988). As shown in Fig. 2, nakhlites have high  $^{129}\text{Xe}/^{132}\text{Xe}$  and low  $^{84}\text{Kr}/^{132}\text{Xe}$  ratios, different from those of shergottites and Chassigny. It was reported that iddingsite is a host phase of the noble gas characteristic of nakhlites; iddingsite in the Lafayette nakhlite (Drake *et al.*, 1994) shows a high  $^{129}\text{Xe}/^{132}\text{Xe}$  (2.04) but a low  $^{84}\text{Kr}/^{132}\text{Xe}$  ratio ( $6 \pm 3$ ) that is clearly lower than that of the Martian atmosphere (20.5; Bogard and Garrison, 1998). It has been inferred that the iddingsite was produced via reactions with water on Mars, and the low  $^{84}\text{Kr}/^{132}\text{Xe}$  ratio might reflect elemental fractionation during the reaction (Drake *et al.*, 1994). On the other hand, Chassigny contains noble gases depleted in lighter elements (Fig. 1), and the  $^{129}\text{Xe}/^{132}\text{Xe}$  is lower than 1.029 and close to the solar value. Other Xe isotope ratios of Chassigny are also similar to those of solar wind (Ott, 1988; Swindle and Jones, 1997; Mathew and Marti, 2001). Chassigny has many petrologic features similar to Earth mantle materials, and hence the compositional characteristics of Chassigny probably represent those of the Mars interior. As shown in Fig. 2, noble gases in shergottites seem to be mixtures of Mars mantle and atmosphere.

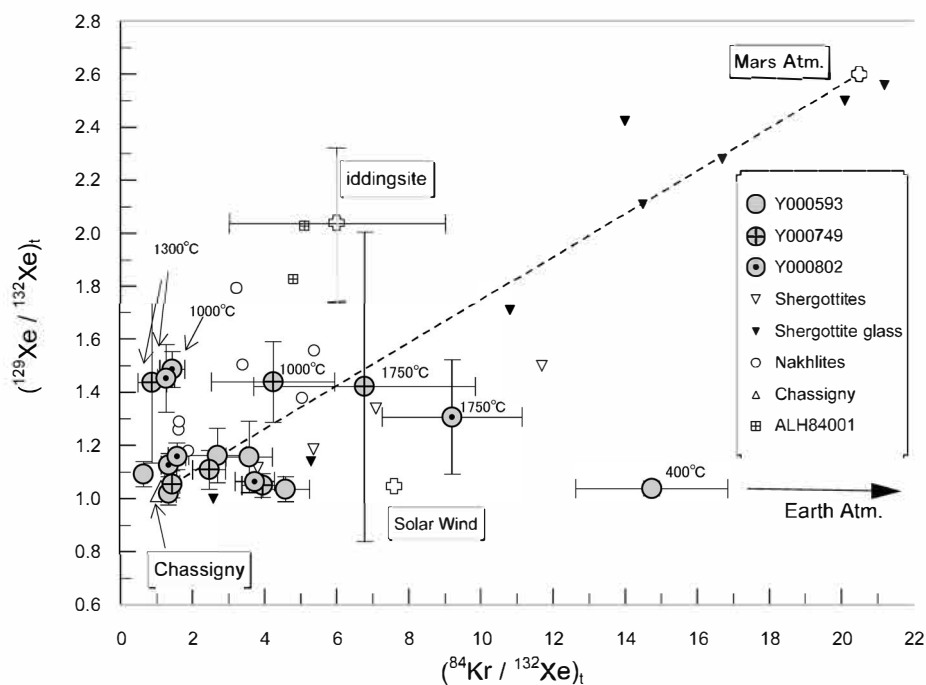


Fig. 2. Plot of  $^{84}\text{Kr}/^{132}\text{Xe}$  versus  $^{129}\text{Xe}/^{132}\text{Xe}$  ratios. Nakhlites contain Chassigny-type and iddingsite noble gases in varying mixing ratios. Data sources: Becker and Pepin (1984, 1993); Bogard and Garrison (1998); Drake *et al.* (1994); Ott (1988); Ott and Löhner (1992); Ott *et al.* (1988); Swindle *et al.* (1986, 1989); Wiens (1988).

Our data show that noble gases released at 1000 and 1300°C from Y000593, Y000749, and Y000802 are similar to those of other non-Antarctic nakhlites, while those at 600 and 800°C are close to Chassigny (Fig. 2 and Table 2). The high  $^{129}\text{Xe}/^{132}\text{Xe}$  and elemental ratios in the high-temperature steps strongly support the petrologic and mineralogical judgment (Imae *et al.*, 2002, 2003) that these meteorites belong to the nakhlite group.

Table 2 and Fig. 3 show isotopic ratios of Xe corrected for the spallation contribution. Noble gases with high  $^{129}\text{Xe}/^{130}\text{Xe}$  ratios released at 1000, 1300, and 1750°C also have excess in  $^{136}\text{Xe}$  (Fig. 3). If noble gases in nakhlites are mixtures between gases in the Mars mantle as found in Chassigny and fractionated atmosphere, as expected from

Table 2. Spallation-corrected Xe isotopes of Y000593, Y000749, and Y000802.

	$^{130}\text{Xe}$	$^{124}\text{Xe}/^{130}\text{Xe}$	$^{126}\text{Xe}/^{130}\text{Xe}$	$^{128}\text{Xe}/^{130}\text{Xe}$	$^{129}\text{Xe}/^{130}\text{Xe}$	$^{131}\text{Xe}/^{130}\text{Xe}$	$^{132}\text{Xe}/^{130}\text{Xe}$	$^{134}\text{Xe}/^{130}\text{Xe}$	$^{136}\text{Xe}/^{130}\text{Xe}$
<i>Y000593 step heating (0.1622g)</i>									
400°C	0.653	0.022	0.0218	0.475	6.90	5.268	6.65	2.569	2.155
	± 0.065	± 0.013	± 0.0046	± 0.014	± 0.13	± 0.090	± 0.12	± 0.064	± 0.041
600°C	0.412	0.023	0.0218	0.445	6.73	5.15	6.49	2.56	2.155
	± 0.041	± 0.015	± 0.0052	± 0.033	± 0.20	± 0.16	± 0.23	± 0.12	± 0.087
800°C	0.895	0.0238	0.0218	0.4623	6.76	5.22	6.62	2.575	2.176
	± 0.090	± 0.0087	± 0.0040	± 0.0083	± 0.13	± 0.12	± 0.25	± 0.071	± 0.055
1000°C	0.177	ND	ND	0.499	7.64	4.78	6.57	2.53	2.17
	± 0.019			± 0.089	± 0.49	± 0.23	± 0.40	± 0.16	± 0.16
1300°C	1.55	0.025	0.022	0.467	7.22	4.96	6.61	2.555	2.237
	± 0.16	± 0.013	± 0.021	± 0.040	± 0.21	± 0.10	± 0.21	± 0.045	± 0.049
1750°C	0.491	ND	ND	0.48	7.72	3.59	6.67	2.48	2.25
	± 0.061			± 0.17	± 0.71	± 0.38	± 0.48	± 0.18	± 0.17
Total	4.18	0.0199	0.0183	0.468	7.10	4.914	6.61	2.552	2.201
	± 0.42	± 0.0058	± 0.0078	± 0.026	± 0.12	± 0.069	± 0.12	± 0.035	± 0.032
<i>Y000593 total melting (0.2953g)</i>									
1750°C	5.70	0.0252	0.022	0.473	7.143	5.053	6.666	2.581	2.219
	± 0.57	± 0.0069	± 0.011	± 0.020	± 0.075	± 0.054	± 0.061	± 0.024	± 0.023
<i>Y000749 step heating (0.2048g)</i>									
400°C	0.763	0.0373	0.0218	0.473	7.00	5.148	6.67	2.543	2.171
	± 0.076	± 0.0095	± 0.0039	± 0.015	± 0.22	± 0.083	± 0.19	± 0.024	± 0.041
600°C	0.488	0.046	0.0218	0.465	7.05	5.17	6.69	2.543	2.179
	± 0.049	± 0.015	± 0.0030	± 0.020	± 0.18	± 0.17	± 0.28	± 0.058	± 0.067
800°C	0.450	0.053	0.0218	0.469	7.39	5.25	6.67	2.58	2.192
	± 0.045	± 0.024	± 0.0080	± 0.031	± 0.30	± 0.14	± 0.34	± 0.12	± 0.046
1000°C	0.111	0.11	ND	0.44	9.69	3.90	6.74	2.47	2.40
	± 0.013	± 0.10		± 0.16	± 0.74	± 0.33	± 0.49	± 0.19	± 0.18
1300°C	0.149	ND	ND	0.44	10.1	2.64	7.0	2.40	2.42
	± 0.028			± 0.37	± 1.5	± 0.59	± 1.0	± 0.36	± 0.40
1750°C	0.104	ND	ND	ND	9.5	ND	6.7	1.98	2.37
	± 0.033				± 2.9		± 1.8	± 0.58	± 0.74
Total	2.06	0.047	ND	0.466	7.59	4.64	6.70	2.509	2.218
	± 0.21	± 0.023		± 0.062	± 0.25	± 0.13	± 0.20	± 0.069	± 0.064
<i>Y000802 step heating (0.1772g)</i>									
400°C	1.45	0.0243	0.0218	0.469	7.07	5.257	6.65	2.597	2.196
	± 0.15	± 0.0030	± 0.0027	± 0.011	± 0.11	± 0.068	± 0.13	± 0.041	± 0.023
600°C	0.567	0.0280	0.0218	0.468	7.48	5.26	6.64	2.616	2.228
	± 0.057	± 0.0066	± 0.0045	± 0.016	± 0.12	± 0.12	± 0.23	± 0.070	± 0.057
800°C	0.496	0.026	0.0218	0.489	7.84	5.28	6.76	2.628	2.254
	± 0.050	± 0.012	± 0.0065	± 0.013	± 0.21	± 0.18	± 0.22	± 0.075	± 0.065
1000°C	0.256	ND	ND	0.470	9.59	4.67	6.46	2.489	2.17
	± 0.026			± 0.053	± 0.31	± 0.16	± 0.21	± 0.078	± 0.07
1300°C	0.310	ND	ND	0.45	9.40	3.65	6.47	2.47	2.29
	± 0.036			± 0.15	± 0.62	± 0.28	± 0.38	± 0.15	± 0.16
1750°C	0.0639	ND	ND	0.49	10.6	3.75	8.09	2.77	2.68
	± 0.0092			± 0.29	± 1.3	± 0.57	± 0.87	± 0.30	± 0.33
Total	3.14	0.0247	0.022	0.471	7.77	5.024	6.66	2.587	2.228
	± 0.32	± 0.0087	± 0.014	± 0.024	± 0.11	± 0.066	± 0.10	± 0.035	± 0.029

Unit for  $^{130}\text{Xe}$  concentration is  $10^{-12} \text{ cm}^3 \text{ STP/g}$ . Presented errors were obtained from propagation of errors for measured isotopic ratios and those for assumed end members. ND: not determined.

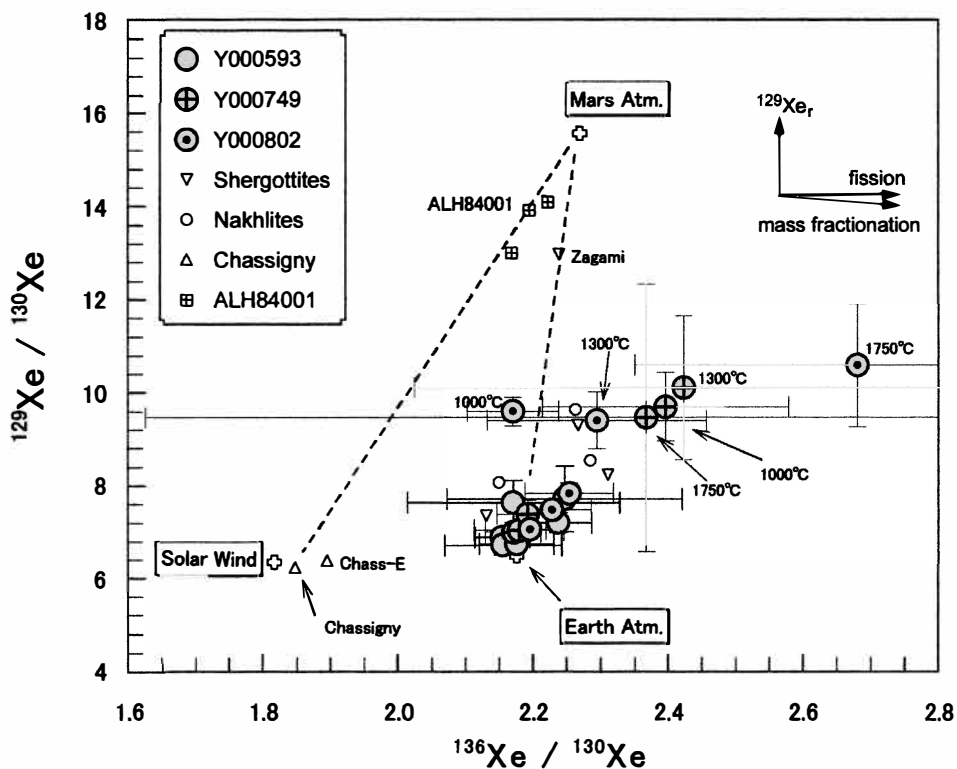


Fig. 3. Spallation-corrected Xe isotopes. High temperature fractions show excesses in  $^{129}\text{Xe}$  and  $^{136}\text{Xe}$ . Data sources: Mathew *et al.* (1998); Miura *et al.* (1995); Ott (1988).

the plot of  $^{129}\text{Xe}/^{132}\text{Xe}$  and  $^{84}\text{Kr}/^{132}\text{Xe}$  (Fig. 2), nakhhlite data should draw a straight line connecting the Mars atmosphere and Chassigny-Xe in Fig. 3. However, no nakhhlite data show such a trend; they plot to the right side of a mixing line between Mars and Earth atmospheres. The rightward shifts from the mixing line suggest that an *in situ* produced fission Xe might be retained in nakhhlites, as suggested by some workers (Ott, 1988; Swindle and Jones, 1997; Mathew and Marti, 2001). On the other hand, there is no simple correlation between fission  $^{136}\text{Xe}$  and excess  $^{129}\text{Xe}$ , which suggests that the excess  $^{129}\text{Xe}$  could come mostly from the Mars atmosphere.

Xenon isotopes of Y000593 show only small excesses in  $^{129}\text{Xe}$  and  $^{136}\text{Xe}$  (Figs. 2 and 3, and Table 2), which is different from those of Y000749 and Y000802. A mineralogical study by Imae *et al.* (2003) found that there is a difference in the modal abundance of olivine; Y000749 and Y000802 contain more abundant olivine phenocrysts than Y000593. This seems reasonable because iddingsite, probably one of the host phases for  $^{129}\text{Xe}$ -rich gas, occurs in rims and fractures in olivine phenocrysts. In addition, Y000593 has a different release pattern of trapped  $^{130}\text{Xe}$  in the step-heating experiment and shows a steep increase of  $^{130}\text{Xe}$  release between 1000 and 1300°C (Table 2). This suggests that a host phase for  $^{130}\text{Xe}$ -rich but  $^{129,136}\text{Xe}$ -poor gas is more abundant in Y000593 than in Y000749 and Y000802. At this time the host phase is not identified,



but it should have high noble gas retentivity.

Low temperature fractions (400–800°C) of the Yamato nakhlites plot around the terrestrial atmosphere (Fig. 3), while Nakhla released noble gases similar to the Chass-E component at 400–500°C (Mathew and Marti, 2002). The Chass-E component is originally determined for high temperature fractions of Chassigny (Mathew *et al.*, 1998). Mathew and Marti (2002) could not exclude a possibility that the Chass-E-like noble gas in Nakhla is a mixture between solar-like Chassigny gas and adsorbed terrestrial atmosphere. Hence, although the Antarctic nakhlites may also contain solar-like noble gas, the indigenous isotopic signature was covered with contamination by fractionated terrestrial gas due to Antarctic weathering. In order to characterize the noble gas released at low temperature we need further investigation on separated minerals with low noble gas retentivity, such as plagioclase and sulfides.

### 3.2. Cosmic-ray exposure (CRE) ages and ejection times from Mars

Timing of ejection from the parent body is the most reliable evidence for source-crater pairing of meteorites. The ejection time is obtained from the sum of CRE and terrestrial ages that are generally estimated from cosmogenic stable and radioactive nuclides of noble gases and other elements such as  $^{10}\text{Be}$ ,  $^{14}\text{C}$ ,  $^{26}\text{Al}$ ,  $^{36}\text{Cl}$ , and  $^{53}\text{Mn}$  (*e.g.*, Nishiizumi, 1987).

Table 3 shows concentrations and isotopic ratios of cosmogenic noble gases, calculated production rates,  $P_{3\text{He}}$ ,  $P_{21\text{Ne}}$ , and  $P_{38\text{Ar}}$ , and CRE ages,  $T_{3\text{He}}$ ,  $T_{21\text{Ne}}$ , and  $T_{38\text{Ar}}$ , based on  $^3\text{He}_c$ ,  $^{21}\text{Ne}_c$ , and  $^{38}\text{Ar}_c$ , respectively. The apparent CRE age ( $T_{81\text{Kr}}$ ), terrestrial age ( $T_t$ ), and ejection time ( $T_e$ ) are also listed. Measured  $^{21}\text{Ne}$  is assumed to be entirely cosmogenic (*i.e.*, no trapped Ne) because Ne isotopic ratios of bulk samples (Appendix) are identical to those of pure spallogenic gases ( $^{20}\text{Ne}/^{22}\text{Ne}\sim 0.8$  and  $^{21}\text{Ne}/^{22}\text{Ne}\sim 0.85$ ). Trapped  $^3\text{He}$  is also negligible because trapped gases, except for solar wind, are generally depleted in light elements (Swindle, 1988). Contributions of trapped  $^{38}\text{Ar}$  were subtracted from the measured  $^{38}\text{Ar}$  concentrations, as mentioned above (Section 2.2). We calculated production rates of  $P_{3\text{He}}$ ,  $P_{21\text{Ne}}$ , and  $P_{38\text{Ar}}$  in the same way as described in Eugster and Michel (1995), using the bulk chemical composition determined for Y000593 (Imae *et al.*, 2003). As shown in Table 3, there are excellent consistencies in the CRE ages between Y000593, Y000749, and Y000802. In addition, cosmogenic  $(^{21}\text{Ne}/^{22}\text{Ne})_c$  and  $(^{78}\text{Kr}/^{83}\text{Kr})_c$  of the three meteorites also show agreement (Table 3), suggesting that these meteorites were irradiated at the similar shielding conditions. These cosmogenic noble gas signatures support the conclusion from the trapped noble gas compositions, petrology, mineralogy, and the find sites (Kojima and Imae, 2001; Kojima *et al.*, 2002; Imae *et al.*, 2002, 2003), that the three Yamato nakhlites were ejected from Mars as a single meteoroid, which broke up at entry to the terrestrial atmosphere.

Mean  $T_{3\text{He}}$  and  $T_{21\text{Ne}}$  ages ( $12.94\pm 0.93$  and  $12.05\pm 0.69$ , respectively) are in good agreement with each other, while  $T_{38\text{Ar}}$  ( $8.46\pm 0.15$ ) disagrees with the other two ages,  $\sim 0.7\times$  shorter. The discrepancy is probably due to uncertainties in corrections of the production rates for variations in chemical compositions and shielding conditions. A recent study by Nishiizumi *et al.* (2002) estimated the production rate for cosmogenic  $^{21}\text{Ne}$  in a basaltic shergottite Dhofar 019 based on radionuclides  $^{10}\text{Be}$ ,  $^{26}\text{Al}$ , and  $^{36}\text{Cl}$ .

Table 3. Concentrations of cosmic ray produced noble gases and calculated cosmic-ray exposure ages of Y000593, Y000749, and Y000802.

	Y000593 (step heating)	Y000593 (total melting)	Y000749 (step heating)	Y000802 (step heating)	
Cosmogenic gases <sup>a)</sup>	<sup>3</sup> He <sub>c</sub>	213	214	209	245
	<sup>21</sup> Ne <sub>c</sub>	20.1	20.9	21.5	24.0
	<sup>38</sup> Ar <sub>c</sub>	16.9	16.4	17.1	16.6
	<sup>81</sup> Kr <sub>c</sub>	-	0.102	-	-
	<sup>83</sup> Kr <sub>c</sub>	8.84	6.43	8.05	5.28
	( <sup>22</sup> Ne/ <sup>21</sup> Ne) <sub>c</sub>	1.206	1.206	1.191	1.184
	( <sup>78</sup> Kr/ <sup>83</sup> Kr) <sub>c</sub>	0.183 ± 0.014	0.1825 ± 0.0089	0.184 ± 0.019	0.179 ± 0.012
	( <sup>81</sup> Kr/ <sup>83</sup> Kr) <sub>c</sub>	-	0.0159 ± 0.0013	-	-
Production rates <sup>b)</sup>	P <sub>3He</sub>	17.0	17.0	17.0	17.1
	P <sub>21Ne</sub>	1.76	1.76	1.81	1.84
	P <sub>38Ar</sub>	1.98	1.98	1.98	1.98
	P <sub>81Kr</sub> /P <sub>83Kr</sub>	-	0.613 ± 0.011	-	-
CRE ages (Ma)	T <sub>3He</sub>	12.6	12.6	12.3	14.3
	T <sub>21Ne</sub>	11.4	11.9	11.9	13.0
	T <sub>38Ar</sub>	8.54	8.29	8.63	8.38
	T <sub>81Kr</sub> <sup>c)</sup>	-	11.8 ± 1.0	-	-
Terrestrial age T <sub>t</sub> (Ma)		<0.04			
Mars ejection time <sup>d)</sup> T <sub>e</sub> (Ma)		12.1 ± 0.7			

<sup>a</sup> Units are in 10<sup>-9</sup> and 10<sup>-12</sup> cm<sup>3</sup> STP/g for He-Ne-Ar, and Kr, respectively.

<sup>b</sup> We estimated production rates for <sup>3</sup>He, <sup>21</sup>Ne, and <sup>38</sup>Ar (P<sub>3He</sub>, P<sub>21Ne</sub>, and P<sub>38Ar</sub>, respectively; shown in 10<sup>-9</sup> cm<sup>3</sup> STP/g/Ma) in the same way as reported in Eugster and Michel (1995) using the bulk composition determined for Y000593 (Imae et al., 2003). The production rate ratio P<sub>81Kr</sub>/P<sub>83Kr</sub> is calculated from an equation in Marti and Lugmair (1971) using (<sup>78</sup>Kr/<sup>83</sup>Kr)<sub>c</sub>.

<sup>c</sup> Apparent CRE age.

<sup>d</sup> Calculated from the sum of T<sub>21Ne</sub> and T<sub>t</sub>.

The Nishiizumi *et al.* (2002) production rate is in agreement with the P<sub>21Ne</sub> calculated for Dhofar 019 in the same way as we used for the Antarctic nakhilites in this study. Therefore, we considered that T<sub>21Ne</sub> is probably the most reliable estimate of the CRE age for these nakhilites.

We also obtained an apparent CRE age (T<sub>81Kr</sub>) for Y000593 based on radioactive <sup>81</sup>Kr and stable Kr isotopes using data in Table 3 and the following equation (Freundel *et al.*, 1986):

$$T_{81Kr} \text{ (yr)} = \frac{1}{\lambda_{81Kr}} \cdot \left( \frac{P_{81Kr}}{P_{83Kr}} \right) \cdot \left( \frac{{}^{83}\text{Kr}}{{}^{81}\text{Kr}} \right)_c,$$

where (P<sub>81Kr</sub>/P<sub>83Kr</sub>) is 1.262 · (<sup>78</sup>Kr/<sup>83</sup>Kr)<sub>c</sub> + 0.381 (Marti and Lugmair, 1971) and λ<sub>81Kr</sub> = 3.25 × 10<sup>-6</sup> yr<sup>-1</sup> (Eastwood *et al.*, 1964). There is no need to input the Kr concentration, which reduces scatter introduced by diffusive gas loss that is often

observed in  $T_{3\text{He}}$ . In addition, the  $T_{81\text{Kr}}$  needs no assumptions on the chemical composition and the shielding condition. The  $T_{81\text{Kr}}$  can be calculated from the production rate ratio ( $P_{81\text{Kr}}/P_{83\text{Kr}}$ ), which is evaluated directly from the Kr isotope spectrum. Hence, the  $T_{81\text{Kr}}$  could be as reliable as the  $T_{21\text{Ne}}$  in determining the CRE age if the terrestrial age of a meteorite is negligible. If  $T_{81\text{Kr}}$  of a meteorite is longer than the appropriate CRE age based on other nuclides, the difference comes from the decay of  $^{81}\text{Kr}$  on the Earth. The obtained  $T_{81\text{Kr}}$  of Y000593 is  $11.8 \pm 1.0$  Ma (Table 3), which agrees with  $T_{21\text{Ne}}$  ( $12.05 \pm 0.69$ ) within the experimental errors. This indicates that the terrestrial age ( $T_t$ ) of the Yamato nakhlites is not long, *i.e.*, the duration of residence in Antarctica should be less than 0.04 Ma (Table 3), which was estimated from the upper-most limit of  $T_{81\text{Kr}}$  and the lowest limit of  $T_{21\text{Ne}}$ . Thus, the ejection time ( $T_e$ ) of the Yamato nakhlites is  $12.1 \pm 0.7$  Ma ago, calculated from the sum of  $T_{21\text{Ne}}$  and  $T_t$ .

Figure 4 plots the cosmogenic  $^{21}\text{Ne}/^{22}\text{Ne}$  ratio against the  $\text{Mg}/(\text{Si} + \text{Al})$  ratio for bulk Martian meteorite samples. The shielding conditions of Y000539, Y000749, and Y000802 (Fig. 4) are similar to those for other non-Antarctic nakhlites (Eugster *et al.*, 1997) that were probably exposed only to galactic cosmic-rays (GCRs). Solar cosmic-ray (SCR) produced Ne has a low  $^{21}\text{Ne}/^{22}\text{Ne}$  (Walton *et al.*, 1976; Hohenberg *et al.*,

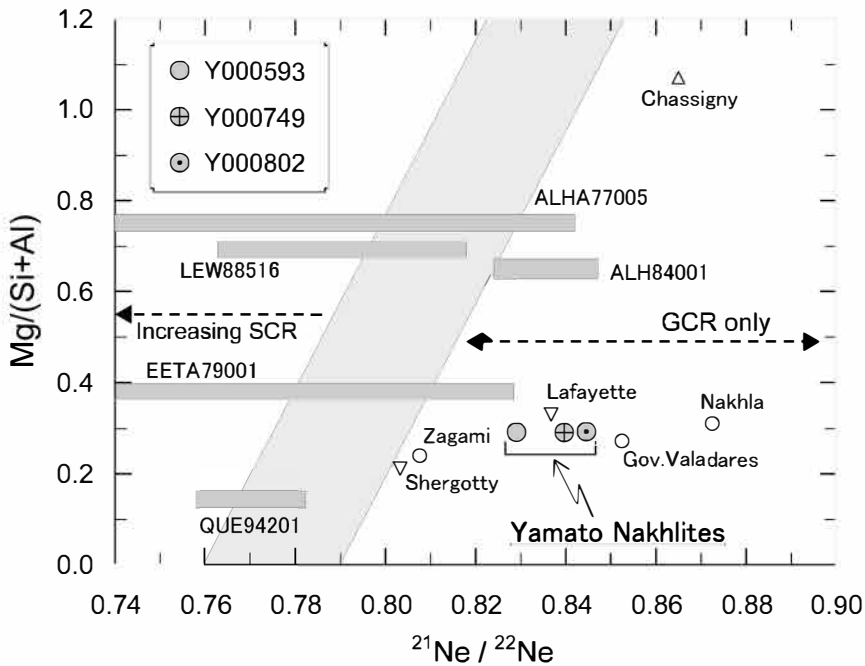


Fig. 4.  $\text{Mg}/(\text{Si} + \text{Al})$  elemental concentration ratios and cosmogenic  $^{21}\text{Ne}/^{22}\text{Ne}$ . The shaded zone represents the boundary between essentially pure GCR-produced Ne on the right and increasing amounts of SCR-produced Ne on the left side, following Begemann and Schultz (1988) and Garrison *et al.* (1995). The slope of the shaded zone was determined using the Bruderheim mineral separates by Garrison *et al.* (1995). Data sources: Bogard *et al.* (1984); Eugster *et al.* (1997); Garrison *et al.* (1995); Miura *et al.* (1995); Swindle *et al.* (1996).

1978; Reedy, 1992) and plots to the left of the boundary (the shaded zone in Fig. 4) between essentially pure GCR-produced Ne and increasing amounts of SCR-produced Ne. The SCR-produced Ne is negligible in the Yamato nakhilites (Fig. 4), although it has been reported for some shergottites (*e.g.*, ALHA77005; Garrison *et al.*, 1995; Miura *et al.*, 1995). Considering the correlation between chemical compositions (Garrison *et al.*, 1995) and shielding conditions (Schultz and Signer, 1976), the measured cosmogenic  $^{22}\text{Ne}/^{21}\text{Ne}$  ratios (1.206, 1.191, and 1.184 for Y000593, Y000749, and Y000802, respectively; Table 3) suggest that the Yamato nakhilites were irradiated by GCRs in a small (<1 m in diameter) pre-atmospheric object. Therefore, we consider that Y000593, Y000749, and Y000802 were ejected directly from Mars by an impact.

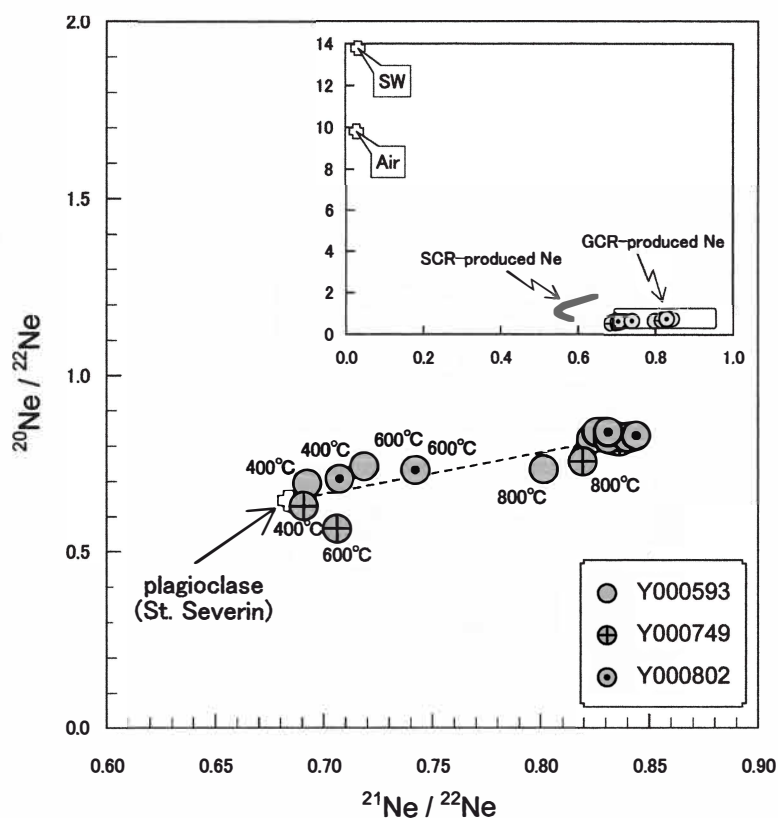


Fig. 5. Neon three isotope plot. Measured  $^{21}\text{Ne}/^{22}\text{Ne}$  ratios elevate as heating temperature increases.

Isotopic ratios of 400°C fractions of the Yamato nakhilites are in excellent agreement with those determined for plagioclase from the St. Severin chondrite (Smith and Huneke, 1975). A range of Ne composition produced via reactions with SCRs is also shown for different shielding conditions (0.5–10 g/cm<sup>2</sup>) and energy spectrum according to Reedy (1992), for the bulk chemical composition of Y000593 (Imae *et al.*, 2003). Isotopic ratios of Ne for terrestrial atmosphere (Air; Ozima and Podosek, 2002) and solar wind (SW; Benkert *et al.*, 1993) are also plotted for comparison.

### 3.3. Cosmogenic Ne produced in Na-rich phases

Step heating analyses revealed that cosmogenic  $^{21}\text{Ne}/^{22}\text{Ne}$  determined at 400 and 600°C are lower (0.69–0.74; Fig. 5 and Appendix) than those released at high temperatures where  $^{21}\text{Ne}/^{22}\text{Ne}$  are normal (GCR-produced Ne). Unlike the case for ALHA77005 shergottite in which the low ( $^{21}\text{Ne}/^{22}\text{Ne}$ )<sub>c</sub> is due to SCR (released at >1200°C; Garrison *et al.*, 1995), the temperature dependent variation in the Yamato nakhlites is due to chemical composition. The low  $^{21}\text{Ne}/^{22}\text{Ne}$  ratios seen for low temperatures (400 and 600°C) in the Yamato nakhlites (Fig. 5) are identical to spallogenic Ne observed in plagioclase separated from the St. Severin chondrite (Smith and Huneke, 1975). High Na content (~6.5 wt%; Smith and Huneke, 1975) is responsible for the low ( $^{21}\text{Ne}/^{22}\text{Ne}$ )<sub>c</sub> of plagioclase, and the Na content of St. Severin plagioclase is similar to those of the Yamato nakhlite plagioclase (~7 wt%; Imae *et al.*, 2003). The  $^{21}\text{Ne}/^{22}\text{Ne}$  ratios at higher temperatures are typical GCR-produced Ne, probably released from olivine and/or augite. Thus, the variations in  $^{21}\text{Ne}/^{22}\text{Ne}$  reflect different minerals with different release temperatures.

### 3.4. Crystallization ages and comparisons with other nakhlites and chassignite

We calculated K-Ar ages for Y000593, Y000749, and Y000802 using the bulk K concentration of 1494 ppm reported for Y000593 (Imae *et al.*, 2003). Table 4 shows K-Ar ages calculated for the Antarctic nakhlites and Nakhla (Ott, 1988) with two assumptions on the trapped  $^{40}\text{Ar}/^{36}\text{Ar}$  ratio. Ott (1988) presented K-Ar age of about 1 Ga for Nakhla assuming negligible contribution of Mars atmospheric Ar, ( $^{40}\text{Ar}/^{36}\text{Ar}$ )<sub>t</sub> = 0. If the same calculation is done for Nakhla assuming that the trapped Ar is present-day Mars atmosphere ( $^{40}\text{Ar}/^{36}\text{Ar}$  = 2000; Owen *et al.*, 1977; Bogard and John-

Table 4. K-Ar ages for Y000593, Y000749, and Y000802.

Sample	K <sup>a</sup> (ppm)	<sup>36</sup> Ar <sub>t</sub>	<sup>(40Ar/36Ar)<sub>t</sub>=0</sup>		<sup>(40Ar/36Ar)<sub>t</sub>=2000</sup>	
			<sup>40</sup> Ar <sub>r</sub>	K-Ar age (Ga)	<sup>40</sup> Ar <sub>r</sub>	K-Ar age (Ga)
Y000593 step heating	1494	2.36	13294	1.48 ±0.14	8574	1.08 ±0.11
Y000593 total melting	1494	0.904	9093	1.13 ±0.12	7285	0.95 ±0.10
Y000749	1494	1.06	11888	1.37 ±0.14	9768	1.19 ±0.12
Y000802	1494	1.60	7669	0.99 ±0.11	4469	0.64 ±0.08
Mean K-Ar age (Ga)				1.24 ±0.22		0.97 ±0.24
Nakhla P1	1378	0.90	7833	1.07 ±0.11	6043	0.88 ±0.10
Nakhla P2/3/4	1378	0.88	7594	1.05 ±0.11	5838	0.85 ±0.10
Nakhla H1	1378	0.86	6511	0.93 ±0.10	4791	0.73 ±0.08

<sup>a</sup> The bulk K concentrations for Y000593 and Nakhla are from Imae *et al.* (2003) and Dreibus *et al.* (1982), respectively.

Concentrations of <sup>36</sup>Ar<sub>t</sub> and <sup>40</sup>Ar<sub>r</sub> are shown in 10<sup>-9</sup> cm<sup>3</sup> STP/g. The Nakhla data are from Ott (1988).

son, 1983), the resulting age is 0.82 Ga, which is  $0.6\times$  younger than those obtained for Nakhla by other radiometric system; 1.3, 1.30, 1.26, and 1.26 Ga are  $^{39}\text{Ar}$ - $^{40}\text{Ar}$ , Rb-Sr, Sm-Nd, and U-Th-Pb ages for Nakhla, respectively (Podosek, 1973; Gale *et al.*, 1975; Papanastassiou and Wasserberg, 1974; Nakamura *et al.*, 1982). Therefore, we calculated K-Ar ages for the Yamato nakhrites assuming a negligible contribution from the Mars atmosphere. The adopted K-Ar age of  $1.24\pm 0.22$  for the Antarctic nakhrites is in agreement with crystallization ages of other nakhrites (around 1.3 Ga; Nyquist *et al.*, 2001 and references therein), although other radiometric ages should be obtained to determine a reliable and precise crystallization age.

The Martian surface consists of rocks with distinct crystallization ages, and has been classified into eight epochs (Tanaka, 1986): Noachian, Hesperian, and Amazonian along with “Early”, “Middle (except for Hesperian)”, and “Late” subdivisions according to the density of impact crater per unit area. The “crater retention age” is related to the evolution of the Martian surface layers to a depth on the order of km (Hartmann and Neukum, 2001), although the ejected Martian rocks are likely to come from shallower surface layers (<several hundred meters; Melosh, 1989). In this context, the combination of the crystallization age and ejection time could discriminate impact events on the Mars surface units.

The ejection times of non-Antarctic nakhrites range between 10.9 and 14.2 Ma (we considered only  $T_{21\text{Ne}}$  for CRE ages reviewed in Nyquist *et al.* (2001) and references therein), while crystallization ages are from 1.27 to 1.34 Ga (Nyquist *et al.*, 2001). Both the crystallization age and ejection time of the Yamato nakhrites are in good agreement with those of other nakhrites. Chassigny also has the ejection time and crystallization age (12.6 Ma and 1.34 Ga; Nyquist *et al.*, 2001) close to those of nakhrites. These chronological data suggest that both Antarctic and non-Antarctic nakhrites, and Chassigny were ejected from a unit of the Martian surface simultaneously by a single impact. One of the possible ejection sites is Amazonis Planitia because the crystallization ages of 1.3 Ga correspond to Early Amazonian epoch according to Hartmann-Tanaka model, as discussed in Nyquist *et al.* (2001). However, the crater retention age has large uncertainties in the time scales of the mid-Martian histories (Hartmann and Neukum, 2001). Thus, it is important to try to identify the original Martian surface units of Martian meteorites by comparison between meteorite samples and Mars exploration data in terms of petrographical, mineralogical and isotopic signatures. Further investigations both on Mars and on Martian meteorites will lead us to understanding the origins and evolution histories of Mars and other terrestrial planets.

#### 4. Summary

We have measured noble gases of Yamato (Y) 000539, Y000749, and Y000802. Calculated cosmic-ray exposure (CRE) ages from cosmogenic He, Ne, and Ar for the three nakhrites are in good agreement with each other;  $T_{21\text{Ne}}$  based on the cosmogenic  $^{21}\text{Ne}$  for Y000593, Y000749, and Y000802 are 11.7, 11.9, and 13.0, respectively. This supports the pairing based on mineralogical and petrographical similarities and the locations of the finds (Kojima and Imae, 2001; Kojima *et al.*, 2002; Imae *et al.*, 2002,

2003). An apparent  $^{81}\text{Kr-Kr}$  age was also determined for Y000593 to be  $11.8 \pm 1.0$  Ma, which agrees with the  $T_{21\text{Ne}}$  within experimental uncertainties. Hence, the terrestrial age of this meteorite should be less than 0.04 Ma. The ejection time was estimated to be  $12.1 \pm 0.7$  Ma. The K-Ar age was calculated as  $1.24 \pm 0.22$  Ga. The ejection time and K-Ar ages are identical to those of other nakhlites and Chassigny.

Trapped noble gas elemental ratios of  $^{36}\text{Ar}/^{84}\text{Kr}/^{132}\text{Xe}$  and  $^{129}\text{Xe}/^{132}\text{Xe}$  indicate that the three Antarctic meteorites are Nakhla-type Martian meteorites. This is also consistent with mineralogical and petrographical studies (Kojima and Imae, 2001; Kojima *et al.*, 2002; Imae *et al.*, 2002, 2003).

Contrary to the similarity in cosmogenic gases, some variations in Xe isotopes were observed among the Antarctic nakhlites. Y000749 and Y000802 show higher contributions of excess  $^{129}\text{Xe}$  and fission  $^{136}\text{Xe}$  compared to Y000593. In addition, the release pattern of trapped  $^{130}\text{Xe}$  for Y000593 is different from those of Y000749 and Y000802. Only Y000593 has enrichment in trapped  $^{130}\text{Xe}$  at high temperature (1300–1750°C). Olivine abundance of Y000593 is also different from those of Y000749 and Y000802 (Imae *et al.*, 2003). These differences in Xe isotopes and petrologic features probably reflect the heterogeneities at the ejection site on the Martian surface.

### Acknowledgments

We thank D.D. Bogard and N. Takaoka for the review comments aiding in the revision of the manuscript. This work was partly supported by the JSPS Research Fellowships for Young Scientists for R.O.

### References

- Anders, E. and Grevesse, N. (1989): Abundances of the elements: Meteoritic and solar. *Geochim. Cosmochim. Acta*, **53**, 197–214.
- Becker, R.H. and Pepin, R.O. (1984): The case for a martian origin of the shergottites: nitrogen and noble gases in EETA 79001. *Earth Planet. Sci. Lett.*, **69**, 225–242.
- Becker, R.H. and Pepin, R.O. (1993): Nitrogen and noble gases in a glass sample from LEW88516. *Lunar and Planetary Science XXIV*. Houston, Lunar Planet. Inst., 77–78.
- Begemann, F. and Schultz, L. (1988): The influence of bulk chemical composition on the production rate of cosmogenic nuclides in meteorites. *Lunar and Planetary Science XIX*. Houston, Lunar Planet. Inst., 51–52.
- Benkert, J.-P., Baur, H., Signer, P. and Wieler, R. (1993): He, Ne, and Ar from the solar wind and solar energetic particles in lunar ilmenites and pyroxenes. *J. Geophys. Res.*, **98** (E7), 13147–13162.
- Bogard, D.D. and Johnson, P. (1983): Martian gases in an Antarctic meteorite? *Science*, **221**, 651–654.
- Bogard, D.D. and Garrison, D.H. (1998): Relative abundances of argon, krypton, and xenon in the Martian atmosphere as measured in Martian meteorites. *Geochim. Cosmochim. Acta*, **62**, 1829–1835.
- Bogard, D.D., Nyquist, L.E. and Johnson, P. (1984): Noble gas contents of shergottites and implications for the Martian origin of SNC meteorites. *Geochim. Cosmochim. Acta*, **48**, 1723–1739.
- Bogard, D.D., Hörz, F. and Johnson, P.H. (1986): Shock-implanted noble gases: an experimental study with implications for the origin of Martian gases in shergottite meteorites. *Proc. Lunar Planet. Sci. Conf.*, 17th, pt. 1, E99–E114 (*J. Geophys. Res.*, **91**, B13).
- Busemann, H. and Eugster, O. (2002): The trapped noble gas component in achondrites. *Meteorit. Planet. Sci.*, **37**, 1865–1891.
- Clayton, R.N. and Mayeda, T.K. (1996): Oxygen isotope studies of achondrites. *Geochim. Cosmochim.*

- Acta, **60**, 1999–2017.
- Drake, M.J., Swindle, T.D., Owen, T. and Musselwhite, D.S. (1994): Fractionated martian atmosphere in the nakhlites? *Meteoritics*, **29**, 854–859.
- Dreibus, G., Palme, H., Rammensee, W., Spettel, B., Weckwerth, G. and Wänke, H. (1982): Composition of Shergotty parent body; Further evidence of a two component model of planet formation. *Lunar and Planetary Science XIII*. Houston, Lunar Planet. Inst., 186–187.
- Eastwood, T.A., Brown, F. and Crocker, I.H. (1964): A krypton-81 half-life determination using a mass separator. *Nuclear Physics*, **58**, 328–336.
- Eberhardt, P., Geiss, J., Graf, H., Grögler, N., Mendia, M.D., Mörgeli, M., Schwaller, H., Steller, A., Krähenbühl, U. and von Gunten, H.R. (1972): Trapped solar wind noble gases in Apollo 12 lunar fines 12001 and Apollo 11 breccia 10046. *Proc. Lunar Sci. Conf.*, 3rd, 1821–1856.
- Eugster, O. and Michel, Th. (1995): Common asteroid break-up events of eucrites, diogenites, and howardites and cosmic-ray production rates for noble gases in achondrites. *Geochim. Cosmochim. Acta*, **59**, 177–199.
- Eugster, O., Weigel, A. and Polnau, E. (1997): Ejection times of Martian meteorites. *Geochim. Cosmochim. Acta*, **61**, 2749–2757.
- Freundel, M., Schultz, L. and Reedy, R.C. (1986): Terrestrial  $^{81}\text{Kr}$ -Kr ages of Antarctic meteorites. *Geochim. Cosmochim. Acta*, **50**, 2663–2673.
- Gale, N.H., Arden, J.W. and Hutchison, R. (1975): The chronology of the Nakhla achondritic meteorite. *Earth Planet. Sci. Lett.*, **26**, 195–206.
- Garrison, D.H., Rao, M.N. and Bogard, D.D. (1995): Solar-proton-produced neon in shergottite meteorites and implications for their origin. *Meteoritics*, **30**, 738–747.
- Geiss, J. and Hess, D.C. (1958): Argon-potassium ages and the isotopic composition of argon from meteorites. *Astrophys. J.*, **127**, 224–236.
- Hartmann, W.K. and Neukum, G. (2001): Cratering chronology and the evolution of Mars. *Space Sci. Rev.*, **96**, 165–194.
- Hohenberg, C.M., Marti, K., Podosek, F.A., Reedy, R.C. and Shirck, J.R. (1978): Comparisons between observed and predicted cosmogenic noble gases in lunar samples. *Proc. Lunar Planet. Sci. Conf.*, 9th, 2311–2344.
- Hudson, G.B., Kennedy, B.M., Podosek, F.A. and Hohenberg, C.M. (1989): The early solar system abundance of  $^{244}\text{Pu}$  as inferred from the St. Severin chondrite. *Proc. Lunar Planet. Sci. Conf.*, 19th, 547–557.
- Imae, N., Okazaki, R., Kojima, H. and Nagao, K. (2002): The first nakhlite from Antarctica. *Lunar and Planetary Science XXXIII*. Houston, Lunar Planet. Inst., #1483 (CD-ROM).
- Imae, N., Ikeda, Y., Shinoda, K., Kojima, H. and Iwata, N. (2003): Yamato nakhlites: Petrography and mineralogy. *Antarct. Meteorite Res.*, **16**, 13–33.
- Kojima, H. and Imae, N., ed. (2001): *Meteorite Newsletter*, **10** (2), 9 p.
- Kojima, H., Nakamura, N., Imae, N. and Misawa, K. (2002): The Yamato nakhlite consortium. *Antarctic Meteorites XXVII*. Tokyo, Natl Inst. Polar Res., 66–68.
- Lugmair, G.W. and Galer, S.J.G. (1992): Age and isotopic relationships among the angrites Lewis Cliff 86010 and Angra dos Reis. *Geochim. Cosmochim. Acta*, **56**, 1673–1694.
- Marti, K., Eberhardt, P. and Geiss, J. (1966): Spallation, fission, and neutron capture anomalies in meteoritic krypton and xenon. *Z. Naturforsch.*, **21a**, 398–413.
- Marti, K. and Lugmair, G.W. (1971):  $\text{Kr}^{81}$ -Kr and  $\text{K}$ -Ar $^{40}$  ages, cosmic-ray spallation products, and neutron effects in lunar samples from Oceanus Procellarum. *Proc. Lunar Sci. Conf.*, 2nd, 1591–1605.
- Mathew, K.J. and Marti, K. (2001): Early evolution of Martian volatiles: Nitrogen and noble gas components in ALH84001 and Chassigny. *J. Geophys. Res.*, **106** (E1), 1401–1422.
- Mathew, K.J. and Marti, K. (2002): Martian atmospheric and interior volatiles in the meteorite Nakhla. *Earth Planet. Sci. Lett.*, **199**, 7–20.
- Mathew, K.J., Kim, J.S. and Marti, K. (1998): Martian atmospheric and indigenous components of xenon and nitrogen in the Shergotty, Nakhla, and Chassigny group meteorites. *Meteorit. Planet. Sci.*, **33**, 655–664.
- McSween, H.Y., Jr. (1994): What we have learned about Mars from SNC meteorites. *Meteoritics*, **29**, 757–



- 779.
- Melosh, H.J. (1989): *Impact Cratering: A Geologic Process*. New York, Oxford Univ. Press, 245 p.
- Miura, Y., Nagao, K. and Fujitani, T. (1993):  $^{81}\text{Kr}$  terrestrial ages and grouping of Yamato eucrites based on noble gas and chemical compositions. *Geochim. Cosmochim. Acta*, **57**, 1857–1866.
- Miura, Y.N., Nagao, K., Sugiura, N., Sagawa, H. and Matsubara, K. (1995): Orthopyroxenite ALH84001 and shergottite ALH77005: Additional evidence for a Martian origin from noble gases. *Geochim. Cosmochim. Acta*, **59**, 2105–2113.
- Miura, Y.N., Nagao, K., Sugiura, N., Fujitani, T. and Warren, P.H. (1998): Noble gases,  $^{81}\text{Kr}$ -Kr exposure ages and  $^{244}\text{Pu}$ -Xe ages of six eucrites, Béréba, Binda, Camel Donga, Juvinas, Millbillillie, and Stannern. *Geochim. Cosmochim. Acta*, **62**, 2369–2387.
- Nagao, K., Okazaki, R., Sawada, S. and Nakamura, N. (1999): Noble gases and K-Ar ages of five Rumuruti chondrites Yamato (Y)-75302, Y-791827, Y-793575, Y-82002, and Asuka-881988. *Antarct. Meteorite Res.*, **12**, 81–93.
- Nakamura, N., Unruh, D.M., Tatsumoto, M. and Hutchison, R. (1982): Origin and evolution of the Nakhla meteorite inferred from the Sm-Nd and U-Pb systematics and REE, Ba, Sr, Rb, and K abundances. *Geochim. Cosmochim. Acta*, **46**, 1555–1573.
- Nishiizumi, K. (1987):  $^{53}\text{Mn}$ ,  $^{26}\text{Al}$ ,  $^{10}\text{Be}$  and  $^{36}\text{Cl}$  in meteorites: Data compilation. *Nucl. Tracks Radiat. Meas.*, **13**, 209–273.
- Nishiizumi, K., Okazaki, R., Park, J., Nagao, K., Masarik, J. and Finkel, R.C. (2002): Exposure and terrestrial histories of Dhofar 019 Martian meteorite. *Lunar and Planetary Science XXXIII*. Houston, Lunar Planet. Inst., #1366 (CD-ROM).
- Nyquist, L.E., Bogard, D.D., Shih, C.-Y., Greshake, A., Stöfler, D. and Eugster, O. (2001): Ages and geological histories of Martian meteorites. *Space Sci. Rev.*, **96**, 105–164.
- Okazaki, R., Takaoka, N., Nagao, K., Sekiya, M. and Nakamura, T. (2001): Noble-gas-rich chondrules in an enstatite meteorite. *Nature*, **412**, 795–798.
- Ott, U. (1988): Noble gases in SNC meteorites: Shergotty, Nakhla, Chassigny. *Geochim. Cosmochim. Acta*, **52**, 1937–1948.
- Ott, U. and Löh, H.P. (1992): Noble gases in the new shergottites LEW 88516 (abstract). *Meteoritics*, **27**, 271.
- Ott, U., Löh, H.P. and Begemann, F. (1988): New noble gas data for SNC meteorites: Zagami, Lafayette, and etched Nakhla (abstract). *Meteoritics*, **23**, 295–296.
- Owen, T., Biemann, K., Rushneck, D.R., Biller, J.E., Howarth, D.W. and Lafleur, L.L. (1977): The composition of the atmosphere at the surface of Mars. *J. Geophys. Res.*, **82**, 4635–4639.
- Ozima, M. and Podosek, F.A. (2002): *Noble Gas Geochemistry*, 2nd ed. Cambridge Univ. Press, 286 p.
- Papanastassiou, D.A. and Wasserburg, G.J. (1974): Evidence for late formation and young metamorphism in the achondrite Nakhla. *Geophys. Res. Lett.*, **1**, 23–26.
- Pepin, R.O. (1985): Evidence of Martian origins. *Nature*, **317**, 473–475.
- Pepin, R.O. (1991): On the origin and early evolution of terrestrial planet atmospheres and meteoritic volatiles. *Icarus*, **92**, 2–79.
- Podosek, F.A. (1973): Thermal history of the nakhrites by the  $^{40}\text{Ar}$ - $^{39}\text{Ar}$  method. *Earth Planet. Sci. Lett.*, **19**, 135–144.
- Reedy, R.C. (1992): Solar-proton production of neon and argon. *Lunar and Planetary Science XXXIII*. Houston, Lunar Planet. Inst., 1133–1134.
- Schultz, L. and Signer, P. (1976): Depth dependence of spallogenic helium, neon, and argon in the St. Severin chondrite. *Earth Planet. Sci. Lett.*, **30**, 191–199.
- Smith, S.P. and Huneke, J.C. (1975): Cosmogenic neon produced from sodium in meteoritic minerals. *Earth Planet. Sci. Lett.*, **27**, 191–199.
- Swindle, T.D. (1988): Trapped noble gases in meteorites. *Meteorites and the Early Solar System*, ed. by J.F. Kerridge and M.S. Matthews. Tucson, Univ. Arizona Press, 535–564.
- Swindle, T.D. and Jones, J.H. (1997): The xenon isotopic composition of the primordial Martian atmosphere: Contributions from solar and fission components. *J. Geophys. Res.*, **102** (E1), 1671–1678.
- Swindle, T.D., Caffee, M.W. and Hohenberg, C.M. (1986): Xenon and other noble gases in shergottites. *Geochim. Cosmochim. Acta*, **50**, 1001–1015.

- Swindle, T.D., Nichols, R. and Olinger, C.T. (1989): Noble gases in the nakhlite Governador Valadares. Lunar and Planetary Science XX. Houston, Lunar Planet. Inst., 1097–1098.
- Swindle, T.D., Li, B. and Kring, D.A. (1996): Noble gases in Martian meteorite QUE94201. Lunar and Planetary Science XXVII. Houston, Lunar Planet. Inst., 1297–1298.
- Tanaka, K.L. (1986): The stratigraphy of Mars. Proc. Lunar Planet. Sci. Conf., 17th, Pt. 1, E139–E158 (J. Geophys. Res. **91**, B13).
- Walton, J.R., Heymann, D. and Yaniv, A. (1976): Production of He, Ne, and Ar isotopes and  $U^{236}$  in lunar materials by solar cosmic ray protons—Production rate calculations. J. Geophys. Res., **81**, 5701–5710.
- Wiens, R.C. (1988): Noble gases released by vacuum crushing of EETA 79001 glass. Earth Planet. Sci. Lett., **91**, 55–65.
- Wiens, R.C. and Pepin, R.O. (1988): Laboratory shock emplacement of noble gases, nitrogen, and carbon dioxide into basalt, and implications for trapped gases in shergottite EETA 79001. Geochim. Cosmochim. Acta, **52**, 295–307.
- Wiens, R.C., Becker, R.H. and Pepin, R.O. (1986): The case for a martian origin of the shergottites, II. Trapped and indigenous gas components in EETA 79001 glass. Earth Planet. Sci. Lett., **77**, 149–158.

*(Received November 8, 2002; Revised manuscript accepted February 3, 2003)*

### Appendix

Concentrations and isotopic ratios of noble gases of Y000593, Y000749, and Y000802. All data are corrected for blank gases and mass discrimination (MD) effects of the mass spectrometer. Concentrations of He, Ne, and Ar are in  $10^{-9}$  cm<sup>3</sup> STP/g, and those of Kr and Xe are in  $10^{-12}$  cm<sup>3</sup> STP/g. Presented errors for isotopic ratios are  $1\sigma$  including statistical errors and errors propagated from the blank and MD corrections. Errors for concentrations are assumed to be 10%.

He, Ne, and Ar isotopes								
	<sup>4</sup> He	<sup>3</sup> He/ <sup>4</sup> He	<sup>22</sup> Ne	<sup>20</sup> Ne/ <sup>22</sup> Ne	<sup>21</sup> Ne/ <sup>22</sup> Ne	<sup>36</sup> Ar	<sup>38</sup> Ar/ <sup>36</sup> Ar	<sup>40</sup> Ar/ <sup>36</sup> Ar
<i>Y000593 step heating (0.1622g)</i>								
400 °C	2041	0.005543 ± 0.000024	0.377	0.704 ± 0.018	0.6924 ± 0.0038	0.154	0.2930 ± 0.0094	841 ± 51
600 °C	2488	0.009760 ± 0.000042	0.102	0.766 ± 0.065	0.718 ± 0.010	0.0758	0.687 ± 0.092	2367 ± 388
800 °C	5535	0.02404 ± 0.00010	0.469	0.743 ± 0.016	0.8015 ± 0.0053	0.579	0.640 ± 0.028	6792 ± 403
1000 °C	550	0.04657 ± 0.00023	3.29	0.8237 ± 0.0037	0.8233 ± 0.0012	0.995	0.677 ± 0.029	7316 ± 418
1300 °C	189	0.08461 ± 0.00077	10.1	0.8408 ± 0.0013	0.82900 ± 0.00062	1.68	1.3172 ± 0.0097	709.8 ± 3.9
1750 °C	21.4	0.145 ± 0.010	10.1	0.8445 ± 0.0018	0.8261 ± 0.0012	9.79	1.4307 ± 0.0022	59.46 ± 0.34
Total	10825	0.019714 ± 0.000060	24.4	0.8357 ± 0.0011	0.82391 ± 0.00060	13.3	1.3078 ± 0.0032	1002 ± 36
<i>Y-000593 total melting (0.2963g)</i>								
1750 °C	8917	0.02400 ± 0.00011	25.3	0.8299 ± 0.0013	0.82579 ± 0.00066	11.5	1.4428 ± 0.0037	791.4 ± 2.0
<i>Y000749 step heating (0.2048g)</i>								
400 °C	1082	0.004587 ± 0.000024	0.226	0.6342 ± 0.0081	0.6912 ± 0.0046	0.104	0.2773 ± 0.0015	802.7 ± 6.5
600 °C	2769	0.009503 ± 0.000069	0.197	0.5706 ± 0.0095	0.7067 ± 0.0035	0.0594	0.928 ± 0.016	3542 ± 69
800 °C	4685	0.02960 ± 0.00014	0.773	0.7611 ± 0.0039	0.8196 ± 0.0016	0.395	1.111 ± 0.026	16587 ± 457
1000 °C	261	0.05601 ± 0.00034	4.11	0.8179 ± 0.0024	0.8366 ± 0.0012	0.321	1.288 ± 0.019	13010 ± 234
1300 °C	198	0.11249 ± 0.00098	11.5	0.8305 ± 0.0021	0.8394 ± 0.0013	1.84	1.4751 ± 0.0031	270.55 ± 0.67
1750 °C	15.1	0.149 ± 0.014	8.90	0.8301 ± 0.0019	0.8371 ± 0.0012	9.36	1.4568 ± 0.0022	38.95 ± 0.14
Total	9010	0.023204 ± 0.000080	25.7	0.8226 ± 0.0012	0.83523 ± 0.00072	12.1	1.4310 ± 0.0020	984 ± 16
<i>Y000802 step heating (0.1772g)</i>								
400 °C	1208	0.008752 ± 0.000039	0.256	0.711 ± 0.018	0.7078 ± 0.0048	0.167	0.2582 ± 0.0026	699 ± 12
600 °C	2733	0.015517 ± 0.000069	0.181	0.737 ± 0.025	0.7428 ± 0.0063	0.0648	0.710 ± 0.040	4071 ± 291
800 °C	3490	0.04329 ± 0.00018	1.24	0.8241 ± 0.0081	0.8315 ± 0.0041	0.644	0.639 ± 0.023	6971 ± 359
1000 °C	227	0.07509 ± 0.00059	5.87	0.8286 ± 0.0018	0.8401 ± 0.0016	0.363	0.900 ± 0.032	6021 ± 272
1300 °C	188	0.1265 ± 0.0012	17.7	0.8342 ± 0.0018	0.8443 ± 0.0015	4.86	1.4695 ± 0.0021	96.22 ± 0.21
1750 °C	1.29	0.397 ± 0.491	3.33	0.8435 ± 0.0036	0.8314 ± 0.0017	6.25	1.4376 ± 0.0015	24.22 ± 0.17
Total	7847	0.03127 ± 0.00012	28.6	0.8320 ± 0.0013	0.8395 ± 0.0010	12.3	1.3730 ± 0.0019	621 ± 20

## Appendix (continued): Kr isotopes

	$^{84}\text{Kr}$	$^{78}\text{Kr}/^{84}\text{Kr}$	$^{80}\text{Kr}/^{84}\text{Kr}$	$^{81}\text{Kr}/^{84}\text{Kr}$	$^{82}\text{Kr}/^{84}\text{Kr}$	$^{83}\text{Kr}/^{84}\text{Kr}$	$^{86}\text{Kr}/^{84}\text{Kr}$
<i>Y000593 step heating (0.1622g)</i>							
400 °C	64.0	0.00627 ± 0.00025	0.03979 ± 0.00067	-	0.2016 ± 0.0011	0.2015 ± 0.0014	0.3073 ± 0.0022
600 °C	12.3	0.00604 ± 0.00038	0.0397 ± 0.0011	-	0.1984 ± 0.0034	0.2024 ± 0.0039	0.3073 ± 0.0031
800 °C	8.04	0.01317 ± 0.00083	0.0621 ± 0.0014	-	0.2280 ± 0.0030	0.2370 ± 0.0037	0.3045 ± 0.0061
1000 °C	4.92	0.103 ± 0.010	0.323 ± 0.031	-	0.561 ± 0.036	0.679 ± 0.046	0.203 ± 0.011
1300 °C	8.15	0.0588 ± 0.0031	0.1953 ± 0.0083	-	0.4036 ± 0.0081	0.465 ± 0.010	0.2577 ± 0.0055
1750 °C	13.7	0.0510 ± 0.0012	0.1696 ± 0.0038	-	0.3663 ± 0.0052	0.4270 ± 0.0064	0.2654 ± 0.0054
Total	111	0.02040 ± 0.00053	0.0814 ± 0.0016	-	0.2543 ± 0.0020	0.2725 ± 0.0025	0.2937 ± 0.0017
<i>Y-000593 total melting (0.2963g)</i>							
1750 °C	155	0.01359 ± 0.00016	0.06129 ± 0.00059	0.000660 ± 0.000043	0.2315 ± 0.0011	0.24048 ± 0.00068	0.3023 ± 0.0016
<i>Y000749 step heating (0.2048g)</i>							
400 °C	20.1	0.00605 ± 0.00022	0.04032 ± 0.00077	-	0.2031 ± 0.0028	0.2009 ± 0.0023	0.3097 ± 0.0030
600 °C	4.73	0.00709 ± 0.00075	0.0404 ± 0.0021	-	0.2059 ± 0.0044	0.2026 ± 0.0024	0.3099 ± 0.0040
800 °C	8.05	0.0325 ± 0.0012	0.1144 ± 0.0060	-	0.291 ± 0.012	0.318 ± 0.012	0.2842 ± 0.0085
1000 °C	5.14	0.105 ± 0.012	0.331 ± 0.036	-	0.577 ± 0.043	0.712 ± 0.069	0.198 ± 0.014
1300 °C	1.84	0.158 ± 0.015	0.474 ± 0.051	-	0.757 ± 0.063	0.934 ± 0.076	0.170 ± 0.017
1750 °C	6.16	0.0788 ± 0.0038	0.251 ± 0.011	-	0.4773 ± 0.0096	0.561 ± 0.022	0.2381 ± 0.0050
Total	46.0	0.0377 ± 0.0016	0.1312 ± 0.0049	-	0.3194 ± 0.0061	0.3562 ± 0.0092	0.2776 ± 0.0027
<i>Y000802 step heating (0.1772g)</i>							
400 °C	36.0	0.00613 ± 0.00021	0.03964 ± 0.00071	-	0.2036 ± 0.0016	0.2030 ± 0.0024	0.3056 ± 0.0021
600 °C	5.23	0.00637 ± 0.00061	0.0417 ± 0.0017	-	0.1990 ± 0.0057	0.1996 ± 0.0040	0.2989 ± 0.0045
800 °C	5.83	0.0260 ± 0.0016	0.0965 ± 0.0031	-	0.2695 ± 0.0058	0.2900 ± 0.0051	0.2809 ± 0.0036
1000 °C	3.30	0.0746 ± 0.0056	0.242 ± 0.015	-	0.457 ± 0.018	0.552 ± 0.031	0.2287 ± 0.0085
1300 °C	3.84	0.1085 ± 0.0041	0.3366 ± 0.0073	-	0.583 ± 0.017	0.709 ± 0.016	0.2141 ± 0.0083
1750 °C	5.40	0.0406 ± 0.0020	0.1396 ± 0.0025	-	0.3292 ± 0.0051	0.3725 ± 0.0062	0.2719 ± 0.0045
Total	59.6	0.02162 ± 0.00049	0.0849 ± 0.0011	-	0.2595 ± 0.0020	0.2785 ± 0.0026	0.2894 ± 0.0016

Appendix (continued):  $^{130}\text{Xe}$ -normalized Xe isotopes

	$^{130}\text{Xe}$	$^{124}\text{Xe}/^{130}\text{Xe}$	$^{126}\text{Xe}/^{130}\text{Xe}$	$^{128}\text{Xe}/^{130}\text{Xe}$	$^{129}\text{Xe}/^{130}\text{Xe}$	$^{131}\text{Xe}/^{130}\text{Xe}$	$^{132}\text{Xe}/^{130}\text{Xe}$	$^{134}\text{Xe}/^{130}\text{Xe}$	$^{136}\text{Xe}/^{130}\text{Xe}$
<b>Y000593 step heating (0.1622g)</b>									
400 °C	0.655	0.024 ± 0.013	0.0254 ± 0.0032	0.478 ± 0.013	6.88 ± 0.13	5.263 ± 0.089	6.63 ± 0.12	2.561 ± 0.064	2.147 ± 0.040
600 °C	0.413	0.023 ± 0.015	0.0230 ± 0.0036	0.446 ± 0.033	6.72 ± 0.20	5.15 ± 0.16	6.48 ± 0.22	2.56 ± 0.12	2.153 ± 0.087
800 °C	0.903	0.0289 ± 0.0084	0.0306 ± 0.0027	0.4713 ± 0.0077	6.71 ± 0.13	5.21 ± 0.12	6.57 ± 0.25	2.555 ± 0.070	2.157 ± 0.054
1000 °C	0.232	0.145 ± 0.021	0.263 ± 0.021	0.737 ± 0.053	6.21 ± 0.32	4.60 ± 0.16	5.22 ± 0.27	1.99 ± 0.11	1.65 ± 0.11
1300 °C	1.88	0.1266 ± 0.0049	0.1979 ± 0.0056	0.646 ± 0.019	6.25 ± 0.14	4.796 ± 0.068	5.62 ± 0.16	2.154 ± 0.025	1.847 ± 0.031
1750 °C	1.02	0.3295 ± 0.0095	0.544 ± 0.014	1.004 ± 0.022	4.58 ± 0.15	3.81 ± 0.10	3.70 ± 0.11	1.328 ± 0.042	1.087 ± 0.031
<b>Total</b>	<b>5.10</b>	0.1291 ± 0.0038	0.2040 ± 0.0037	0.653 ± 0.0093	6.114 ± 0.071	4.752 ± 0.043	5.585 ± 0.081	2.138 ± 0.022	1.805 ± 0.019
<b>Y-000593 total melting (0.2963g)</b>									
1750 °C	6.41	0.0903 ± 0.0013	0.1345 ± 0.0016	0.5874 ± 0.0055	6.529 ± 0.027	4.938 ± 0.034	6.025 ± 0.034	2.321 ± 0.014	1.972 ± 0.013
<b>Y000749 step heating (0.2048g)</b>									
400 °C	0.763	0.0373 ± 0.0093	0.0219 ± 0.0028	0.473 ± 0.015	7.00 ± 0.21	5.148 ± 0.083	6.67 ± 0.19	2.543 ± 0.023	2.171 ± 0.041
600 °C	0.489	0.047 ± 0.015	0.0232 ± 0.0021	0.467 ± 0.020	7.04 ± 0.18	5.17 ± 0.17	6.68 ± 0.28	2.540 ± 0.058	2.176 ± 0.066
800 °C	0.462	0.067 ± 0.023	0.0473 ± 0.0053	0.495 ± 0.029	7.25 ± 0.29	5.22 ± 0.13	6.52 ± 0.33	2.52 ± 0.11	2.137 ± 0.043
1000 °C	0.214	0.349 ± 0.046	0.506 ± 0.016	0.947 ± 0.036	5.84 ± 0.18	3.956 ± 0.096	3.95 ± 0.16	1.411 ± 0.063	1.249 ± 0.051
1300 °C	0.416	0.406 ± 0.025	0.669 ± 0.040	1.115 ± 0.077	4.68 ± 0.11	3.525 ± 0.061	3.12 ± 0.11	1.025 ± 0.049	0.872 ± 0.047
1750 °C	0.489	0.488 ± 0.022	0.817 ± 0.043	1.279 ± 0.036	3.305 ± 0.079	3.038 ± 0.074	2.141 ± 0.097	0.623 ± 0.050	0.506 ± 0.036
<b>Total</b>	<b>2.83</b>	0.1993 ± 0.0081	0.2952 ± 0.0097	0.745 ± 0.015	5.981 ± 0.085	4.470 ± 0.046	5.137 ± 0.092	1.899 ± 0.025	1.618 ± 0.020
<b>Y000802 step heating (0.1772g)</b>									
400 °C	1.45	0.0247 ± 0.0028	0.0226 ± 0.0019	0.470 ± 0.011	7.06 ± 0.11	5.256 ± 0.068	6.64 ± 0.13	2.595 ± 0.040	2.194 ± 0.023
600 °C	0.567	0.0283 ± 0.0063	0.0223 ± 0.0031	0.469 ± 0.015	7.48 ± 0.12	5.26 ± 0.12	6.64 ± 0.23	2.614 ± 0.069	2.227 ± 0.057
800 °C	0.507	0.039 ± 0.011	0.0443 ± 0.0043	0.512 ± 0.012	7.70 ± 0.21	5.25 ± 0.17	6.63 ± 0.22	2.575 ± 0.072	2.203 ± 0.063
1000 °C	0.333	0.156 ± 0.012	0.257 ± 0.013	0.709 ± 0.014	7.74 ± 0.15	4.52 ± 0.10	5.17 ± 0.12	1.969 ± 0.041	1.666 ± 0.029
1300 °C	0.592	0.2994 ± 0.0095	0.501 ± 0.013	0.947 ± 0.029	5.718 ± 0.063	3.828 ± 0.042	3.838 ± 0.084	1.418 ± 0.035	1.207 ± 0.044
1750 °C	0.152	0.371 ± 0.029	0.606 ± 0.025	1.072 ± 0.080	5.41 ± 0.32	3.91 ± 0.17	3.94 ± 0.19	1.315 ± 0.061	1.131 ± 0.077
<b>Total</b>	<b>3.60</b>	0.0992 ± 0.0031	0.1505 ± 0.0028	0.6016 ± 0.0079	6.991 ± 0.061	4.896 ± 0.043	5.929 ± 0.072	2.290 ± 0.023	1.945 ± 0.018

Appendix (continued):  $^{132}\text{Xe}$ -normalized Xe isotopes

	$^{132}\text{Xe}$	$^{124}\text{Xe}/^{132}\text{Xe}$	$^{126}\text{Xe}/^{132}\text{Xe}$	$^{128}\text{Xe}/^{132}\text{Xe}$	$^{129}\text{Xe}/^{132}\text{Xe}$	$^{130}\text{Xe}/^{132}\text{Xe}$	$^{131}\text{Xe}/^{132}\text{Xe}$	$^{134}\text{Xe}/^{132}\text{Xe}$	$^{136}\text{Xe}/^{132}\text{Xe}$
<i>Y000593 step heating (0.1622g)</i>									
400 °C	4.34	0.0036 ± 0.0019	0.00384 ± 0.00051	0.0723 ± 0.0019	1.040 ± 0.016	0.1509 ± 0.0023	0.794 ± 0.011	0.3845 ± 0.0086	0.3220 ± 0.0046
600 °C	2.67	0.0036 ± 0.0025	0.00355 ± 0.00058	0.0689 ± 0.0034	1.037 ± 0.024	0.1543 ± 0.0049	0.794 ± 0.016	0.393 ± 0.012	0.3299 ± 0.0061
800 °C	5.92	0.0044 ± 0.0014	0.00467 ± 0.00036	0.0720 ± 0.0016	1.024 ± 0.013	0.1525 ± 0.0047	0.7905 ± 0.0078	0.3876 ± 0.0062	0.3268 ± 0.0044
1000 °C	1.21	0.0277 ± 0.0040	0.0505 ± 0.0048	0.1413 ± 0.0097	1.188 ± 0.045	0.1913 ± 0.0077	0.881 ± 0.024	0.378 ± 0.015	0.314 ± 0.017
1300 °C	10.5	0.02258 ± 0.00071	0.03528 ± 0.00063	0.1152 ± 0.0019	1.1126 ± 0.0069	0.1782 ± 0.0045	0.843 ± 0.010	0.3807 ± 0.0045	0.3261 ± 0.0048
1750 °C	3.76	0.0897 ± 0.0026	0.1478 ± 0.0042	0.2722 ± 0.0063	1.241 ± 0.024	0.2707 ± 0.0081	1.033 ± 0.024	0.3587 ± 0.0093	0.2931 ± 0.0060
Total	28.5	0.02320 ± 0.00068	0.03665 ± 0.00065	0.1172 ± 0.0013	1.0981 ± 0.0062	0.1782 ± 0.0022	0.8469 ± 0.0057	0.3808 ± 0.0031	0.3211 ± 0.0024
<i>Y-000593 total melting (0.2963g)</i>									
1750 °C	38.6	0.01513 ± 0.00025	0.02247 ± 0.00019	0.09793 ± 0.00094	1.0872 ± 0.0042	0.16633 ± 0.00094	0.8215 ± 0.0049	0.3858 ± 0.0020	0.3271 ± 0.0021
<i>Y000749 step heating (0.2048g)</i>									
400 °C	5.06	0.0057 ± 0.0015	0.00333 ± 0.00041	0.0716 ± 0.0015	1.057 ± 0.022	0.1507 ± 0.0032	0.788 ± 0.018	0.3871 ± 0.0044	0.3298 ± 0.0067
600 °C	3.25	0.0071 ± 0.0022	0.00351 ± 0.00035	0.0703 ± 0.0025	1.060 ± 0.016	0.1503 ± 0.0051	0.779 ± 0.013	0.384 ± 0.010	0.3284 ± 0.0065
800 °C	3.00	0.0104 ± 0.0034	0.00729 ± 0.00081	0.0762 ± 0.0040	1.115 ± 0.026	0.1539 ± 0.0057	0.804 ± 0.021	0.389 ± 0.013	0.3289 ± 0.0056
1000 °C	0.840	0.090 ± 0.011	0.1295 ± 0.0057	0.2415 ± 0.0094	1.486 ± 0.038	0.2543 ± 0.0073	1.012 ± 0.030	0.362 ± 0.016	0.320 ± 0.014
1300 °C	1.29	0.1318 ± 0.0084	0.216 ± 0.015	0.360 ± 0.025	1.510 ± 0.054	0.3218 ± 0.0097	1.140 ± 0.040	0.333 ± 0.012	0.283 ± 0.015
1750 °C	1.05	0.230 ± 0.012	0.384 ± 0.028	0.600 ± 0.032	1.549 ± 0.048	0.468 ± 0.018	1.426 ± 0.043	0.293 ± 0.015	0.238 ± 0.014
Total	14.5	0.0393 ± 0.0017	0.0580 ± 0.0025	0.1460 ± 0.0034	1.170 ± 0.012	0.1954 ± 0.0025	0.8797 ± 0.0096	0.3738 ± 0.0043	0.3179 ± 0.0035
<i>Y000802 step heating (0.1772g)</i>									
400 °C	9.61	0.00380 ± 0.00044	0.00343 ± 0.00030	0.0712 ± 0.0014	1.068 ± 0.011	0.1510 ± 0.0023	0.7983 ± 0.0082	0.3920 ± 0.0052	0.3308 ± 0.0029
600 °C	3.75	0.00443 ± 0.00094	0.00340 ± 0.00049	0.0712 ± 0.0023	1.133 ± 0.020	0.1513 ± 0.0041	0.797 ± 0.018	0.397 ± 0.014	0.3375 ± 0.0099
800 °C	3.35	0.0060 ± 0.0016	0.00675 ± 0.00065	0.0777 ± 0.0022	1.167 ± 0.022	0.1513 ± 0.0041	0.798 ± 0.016	0.3909 ± 0.0084	0.3337 ± 0.0077
1000 °C	1.72	0.0306 ± 0.0023	0.0499 ± 0.0024	0.1364 ± 0.0018	1.601 ± 0.022	0.1937 ± 0.0033	0.871 ± 0.018	0.380 ± 0.012	0.3208 ± 0.0076
1300 °C	2.26	0.0791 ± 0.0024	0.1318 ± 0.0034	0.2483 ± 0.0063	1.497 ± 0.028	0.2614 ± 0.0042	1.002 ± 0.016	0.3720 ± 0.0061	0.316 ± 0.010
1750 °C	0.594	0.0976 ± 0.0053	0.1572 ± 0.0047	0.276 ± 0.019	1.388 ± 0.045	0.256 ± 0.011	1.022 ± 0.033	0.345 ± 0.015	0.295 ± 0.015
Total	21.3	0.01705 ± 0.00050	0.02564 ± 0.00048	0.1020 ± 0.0012	1.1927 ± 0.0078	0.1692 ± 0.0015	0.8317 ± 0.0060	0.3884 ± 0.0038	0.3290 ± 0.0028